ACTA PHYSICA SINICA
Volume 2, Number 4 (Overseas Edition) April, 1993

SIZE EFFECT OF INNER RADIUS ON CIRCULARLY SYMMETRIC SOLITON STATES IN ANNULAR JOSEPHSON JUNCTIONS*

XU KUN-MING (徐昆明) and LU DAO-FANG (陆道芳)
Department of Physics, Zhejiang University, Hangzhou 310027, China

YAO XI-XIAN (姚希贤)
Department of Physics, Nanjing University, Nanjing 210008, China

(Received 1 June 1992)

The effect of the inner radius of an annular Josephson junction on the excitation of circularly symmetric soliton states is explored by direct numerical simulation. In a circularly symmetric annular Josephson junction (CSAJJ hereafter), the phase difference in the order parameters Φ across the junction barrier obeys the modified sine-Gordon equation (SGE) in which there is a perturbation term Φ_p/ρ inversely proportional to the radial coordinate ρ, and this term does not appear in the case of a 1D in-line junction. The effect of the Φ_p/ρ term becomes prominent when ρ is small. It turns out that for junctions of given dissipation and annular width, there is a lower limit of the inner radii for the junctions to support stable soliton motion, while the lower limit depends strongly on the dissipation coefficient α. For example, for a CSAJJ with inner radius $5\lambda_J$, outer radius $10\lambda_J$, no stable soliton states would exist when $\alpha=0.01$ or $\alpha=0.02$. However, for $0.06\geqslant\alpha\geqslant0.03$, there are ring-shaped solitary wave solutions, presumably because the dissipation suppresses the effect of the Φ_p/ρ term. Finally, the behaviour of the soliton states and the relevant I-V characteristics are also discussed.

PACC: 7450; 0340K

I. INTRODUCTION

As a diverse nonlinear physical system, the Josephson junction has been attracting much attention, not only because it is a good model for studies of nonlinear dynamical systems, but also because it has a wide range of physical application, e.g., as a basic unit of superconducting microelectronic devices. For 1D long Josephson junctions there have been found many theoretical and experimental researches in the literature[1-5] on fluxon (or soliton) oscillation. The radiation power of a 1D junction is relatively small, and this makes the coupling of the junction with the external devices difficult. It was argued that a number of properly coupled junctions might generate larger power[5]. Studies have also been made on 2D junctions with rectangular and circular geometry (see Ref. [1] and Refs. [6-8] respectively). Particularly, we note that Christiansen *et al.*[7] have discussed a practical model for the application of a circular Josephson junction, and Maslov[6, 8] has

* Project supported by the National Natural Science Foundation of China.

investigated the rotationally symmetric soliton motion by perturbation treatments. The authors in, for example, Ref. [9] pointed out earlier that stable circularly symmetric soliton solutions may exist if one adopts the CSAJJ model. Geometrically, one obtains a CSAJJ by rotating 1D in-line junction about the origin which is on the extended length axis of the in-line junction, with the rotation axis perpendicular to the length axis. Therefore, an annular junction is equivalent to an infinite number of parallelly coupled in-line junctions, and it could generate a larger output radiation power than that of an in-line junction.

From numerical simulation[9-11] the soliton behaviour in annular junctions with dissipation coefficient $\alpha=0.01$ and different sizes is described as follows. Soliton solutions can be achieved when $\rho_0 \geqslant 7.5\lambda_J$ (ρ_0 is the inner radius of the junction); with the increase of ρ_0, e.g., $\rho_0=50\lambda_J$, the soliton behaves essentially like the one in a 1D overlap junction[3]. Recently, Wang *et al.*[12] perturbatively investigated the soliton motion in modified sine-Gordon equation (SGE) of annular junctions, and suggested that as long as $\rho_0 \geqslant 5\lambda_J$, a particle model of soliton is plausible. For further understanding of the soliton behaviour, it is necessary to explore the condition, or the lower limit of the inner radius ρ_0 for the junction to support a stable soliton motion. And this will examine the validity of the particle model on one hand, and will provide a background for the research of other physical systems that would support circularly symmetric soliton (CS soliton hereafter) excitations on the other hand. (Examples are dislocation rings in semiconductors[13] and rotationally symmetric domain walls in ferromagnetic materials[14].)

The CSAJJ is described by the modified SGE[9-11]

$$\Phi_{\rho\rho}+\Phi_\rho/\rho-\Phi_{tt}=\alpha\Phi_t+\sin\Phi, \tag{1}$$

where ρ is the radial coordinate, Φ the phase difference of the order parameters of the superconductors across the oxide barrier. The term $\alpha\Phi_t$ in Eq. (1) results from the quasiparticle tunnelling, and is dissipative. The normalization of Eq. (1) can be found, for example, in Ref. [9]. Note that all the quantities are dimensionless hereafter.

The current I_H which provides a symmetric external magnetic field for the junction flows along another conducting wire located at the center of the junction. The current I_H and the driving current of the junction I will affect the behaviour of the junction through the boundary conditions[9]

$$\begin{aligned}\Phi_\rho(\rho=\rho_0)&=I_H/2\pi\ \rho_0,\\ \Phi_\rho(\rho=\rho_1)&=(I_H+I)/2\pi\ \rho_1,\end{aligned} \tag{2}$$

where ρ_0 and ρ_1 are the inner and outer radii respectively.

II. NUMERICAL SIMULATION

A. $\alpha=0.01$ (see also Refs. [9] and [10])

We now discuss the case of zero applied magnetic field, i.e., $I_H=0$. The initial condition in solving Eq. (1) is chosen to be the SG soliton solution $U=(\Phi, \Phi_t)$,

$$\Phi(\rho,\ 0)=4\arctan\ \exp\frac{\rho-\rho_c}{(1-v^2)^{1/2}}\ ,$$

$$\Phi_t(\rho,\ 0)=\frac{-2v}{(1-v^2)^{1/2}}\ \mathrm{sech}\frac{\rho-\rho_c}{(1-v^2)^{1/2}}\ , \tag{3}$$

where ρ_c is the initial center position of the soliton, and v the initial velocity.

First, we choose $\rho_0=7.5$, $\rho_1=12.5$, $\rho_c=11.5$ and $v=0.9$. Follwing the approach described in Ref. [9] (with space step length 0.05 and time step length 0.01), we obtain the I'-$\langle V\rangle$ characteristics of the junction in the lower voltage regime, as shown in Fig. 1 (solid lines). I' is the renormalized driving current $I'=I/\pi\ (\rho_1^2-\rho_0^2)$, and $\langle V\rangle=\Delta\Phi/T$, where $\Delta\Phi$ is the change of Φ during a temporal interval T, T being the period of the soliton oscillation. Three zero field steps (ZFS) have been observed, and the ratio of the corresponding voltages is 1:2:3. The step with the lowest voltage is related to single soliton oscillations (travelling wave solutions), and a Φ_ρ-ρ-t curve is shown in Fig. 2(a). The other two steps correspond to 2-soliton and 3-soliton standing wave solutions, and their Φ_ρ-ρ-t curves are shown in Figs. 2(b) and 2(d) respectively. Figures 2(c) and 2(e) are the local blow-up of Figs. 2(b) and 2(d), respectively, along the t-axis. These solutions resemble the symmetric 2-soliton and 3-soliton solutions in a 1D junction obtained by Lomdahl *et al.*[3]. In addition, the hysteresis feature in Fig. 1 is evident. The initial condition for calculating 2-soliton solutions are

$$\Phi(\rho,\ 0)=4\arctan\ \exp\frac{\rho-\rho_{c1}}{(1-v_1^2)^{1/2}}\ +4\arctan\ \exp\frac{\rho-\rho_{c2}}{(1-v_2^2)^{1/2}}\ ,$$

$$\Phi_t(\rho,\ 0)=\frac{-2v_1}{(1-v_1^2)^{1/2}}\ \mathrm{sech}\frac{\rho-\rho_{c1}}{(1-v_1^2)^{1/2}}-\frac{-2v_2}{(1-2v_2^2)^{1/2}}\ \mathrm{sech}\frac{\rho-\rho_{c2}}{(1-v_2^2)^{1/2}}\ , \tag{4}$$

where $\rho_{c1}=8.5$, $\rho_{c2}=11.5$ and $v_1=v_2=0.9$.

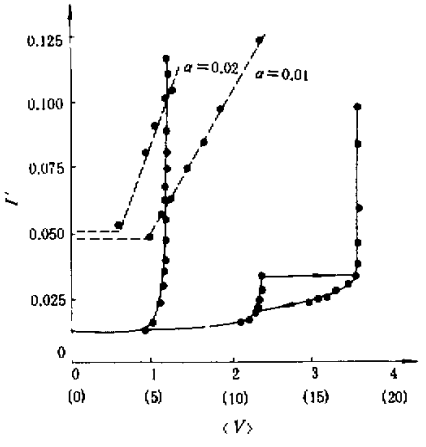

Fig. 1. I'-$\langle V\rangle$ characteristics of the annular junctions. Solid lines: $\rho_0=7.5$, $\rho_1=12.5$ and $\alpha=0.01$; Dashed lines: $\rho_0=5$, $\rho_1=10$, $\alpha=0.01$ and $\alpha=0.02$ (see the text).

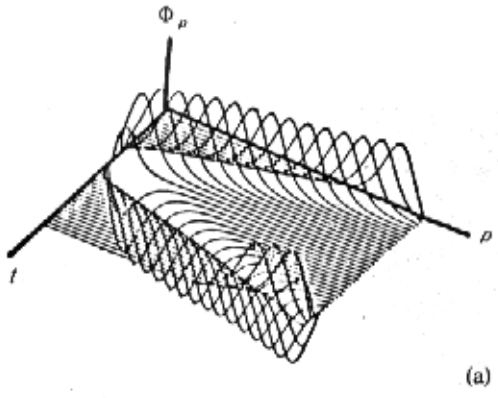

(a)

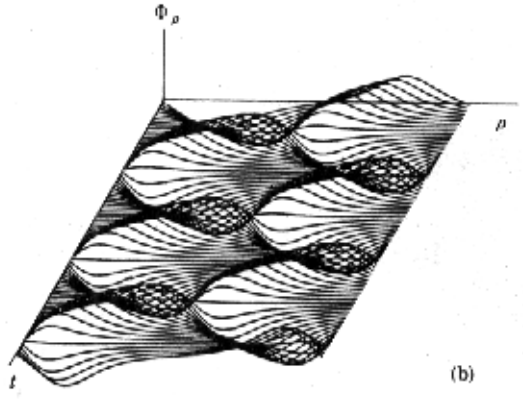

(b)

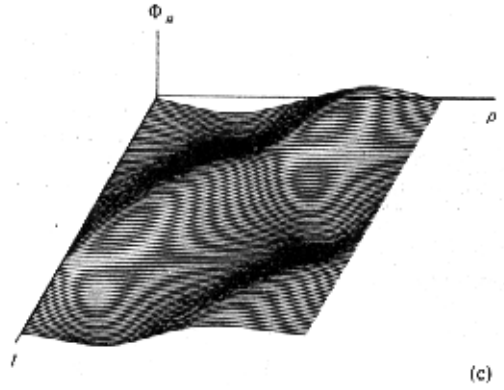

(c)

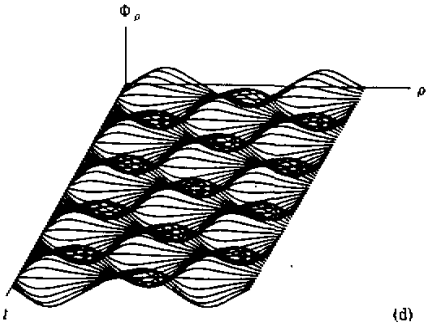

(d)

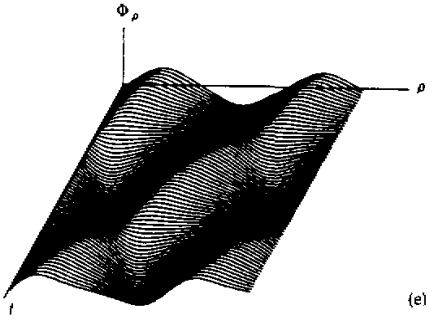

(e)

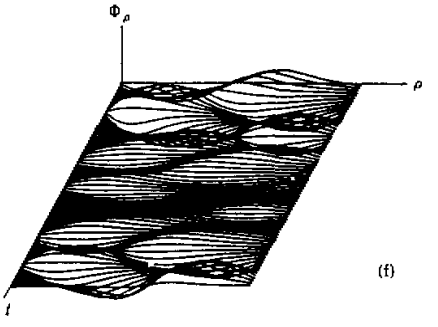

(f)

Fig. 2(a)–2(f). Φ_ρ-ρ-t curves for junctions with $\alpha=0.01$, $\rho_0=7.5$ and $\rho_1=12.5$. (a): Travelling wave solution with single soliton excitation; (b) and (d): standing wave solutions with 2-soliton and 3-soliton excitations, respectively; (c) and (e): the local blow-up of (b) and (d), respectively, along the t-axes; (f): Φ_ρ-ρ-t curve for a junction with $\alpha=0.01$, $\rho_0=5$ and $\rho_1=10$. The driving current is $I=0.045$. The time t runs from $t=900$ after the starting of simulation. The solution tends to zero voltage state at $t=1450$.

Next, we choose $\rho_0=5$, $\rho_1=10$. The stable soliton solution obtained above is taken to be the initial condition here. It turns out that the final state is either zero voltage state or periodic rotational state, and the single soliton state is transient and unstable. The rotational state switches to zero voltage state in the current range of $0.045<I'<0.050$, as has been shown in Fig. 1(dashed lines). Note the scale is changed here, and $\langle V\rangle$ is given in brackets for the dashed lines.

By comparison, the only difference between the two junctions we have studied so far is the inner radius difference of 2.5. However, for a smaller ρ_0, a soliton is perturbed or distorted more remarkably when it reaches the inner boundary. Figure 2(f) shows the solution after $t=900$, with the driving current $I'=0.045$. The solution resembles that in Fig. 2(b) at the first sight, but it is unstable, and tends to zero voltage state at $t=1450$.

It is, therefore, obvious that for an underdamped annular junction, the soliton behaviour depends strongly upon the inner radius.

B. $\alpha=0.05$

Again, with the soliton solution with $\rho_0=7.5$, $\rho_1=12.5$ and $\alpha=0.01$ as the initial condition, we investigate numerically the soliton in a junction with $\alpha=0.05$, $\rho_0=7.5$ and $\rho_1=12.5$, and another one with $\alpha=0.05$, $\rho_0=5$ and $\rho_1=10$. Under this dissipation, both of these junctions exhibit first, second and third ZFSs, as shown in Figs. 3(a) and 3(b). The oblique lines in Fig. 3 are the Ohmic current-voltage relations, on which all rotational states rest. Notable is the switching from 2-ZFS at $I'=0.090$ when I' decreases along the

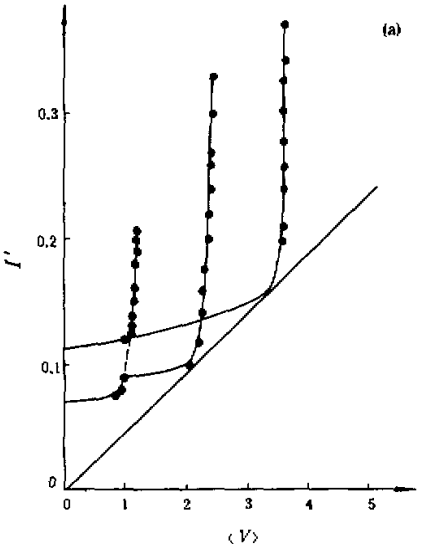

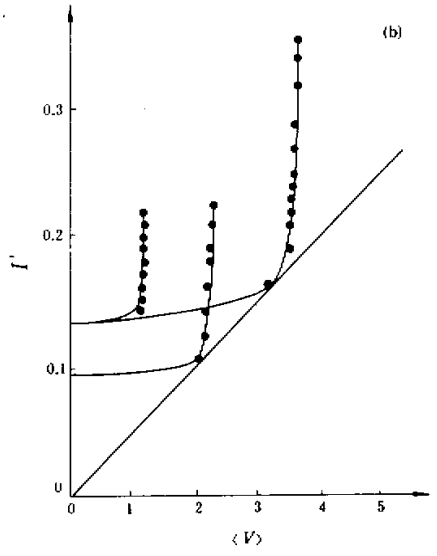

Fig. 3. I'-$\langle V \rangle$ characteristics for $\alpha=0.05$: (a) $\rho_0=7.5$, $\rho_1=12.5$; (b) $\rho_0=5$, $\rho_1=10$.

2-ZFS, and it corresponds to the intermediate state when switching from a 2-soliton state to a single soliton state, and the resultant soliton state is stable in the current range $0.090 \geqslant I' \geqslant 0.075$, which is on the extended portion of the upper 1-ZFS. And in the current range $0.090 < I' < 0.120$, we have so far found only zero voltage state. Further investigation is deserved of what the mechanism would be if the current gap on the 1-ZFS is inherent to the junction itself.

C. Other values of α

We take the soliton solution $U=(\Phi, \Phi_t)$ with $\rho_0=5$, $\rho_1=10$ and $\alpha=0.05$ as the initial condition to explore the soliton excitations under other dissipations, $\alpha=0.04$ and $\alpha=0.06$. The resultant soliton solutions are again taken as initial conditions for slightly different α. The 1-ZFSs for α in the range $0.06 \geqslant \alpha \geqslant 0.03$ are plotted in Fig. 4. These results show that the lower limit of the inner radius would depend strongly on the dissipation. Interestingly, we find in numerical experiments that for $\alpha > 0.06$, single soliton state becomes unstable; however, 2-soliton state remains stable. This is the case at least up to $\alpha=0.10$. Recalling the transient 2-soliton solution in Fig. 2(f) when the single soliton state loses stability at $\alpha=0.01$, we conjecture that with the increase of α to a certain extent the boundary conditions [see Eq. (2)] favour the excitation of 2-soliton standing wave solutions instead of single soliton travelling solutions. The I'-$\langle V \rangle$ characteristics for $\alpha=0.02$ is also shown in Fig. 1 (the dashed line with a larger slope).

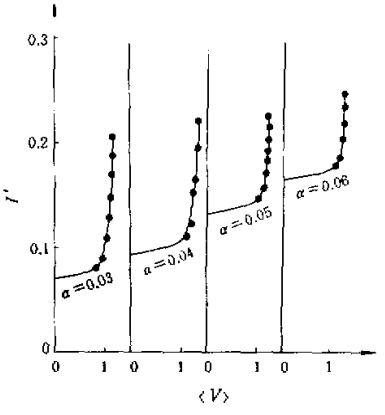

Fig. 4. The I-ZFSs of the junction with $\rho_0=5$, $\rho_1=10$ and various dissipation. The $\langle V\rangle$-axis is offset to the right successively for $\alpha=0.03$, 0.04, 0.05 and 0.06.

III. DISCUSSION

For the very small dissipation, e.g., $\alpha=0.01$, the annular junction with $\rho_0=7.5$ and $\rho_1=12.5$ exhibits three branches of ZFSs, but the junction with $\rho_0=5$ and $\rho_1=10$ supports no stable soliton solution. Therefore, the $1/\rho$ term in Eq. (1) affects the soliton behaviour prominently. Our results show that the particle model of soliton is invalid if one deals with the junctions of sizes under present consideration, although it might be theoretically plausible.

Investigation of soliton energy E and velocity v would strengthen our conclusion. Figures 5 (a) and 5 (b) show the E-ρ_c curve and v-ρ_c curve for $\alpha=0.01$ and $\alpha=0.05$ respectively, where ρ_c is the center position of the soliton. The size parameters are $\rho_0=7.5$ and $\rho_1=12.5$. Figure 5(a) is obtained in the following manner. For $I'=0.068$, the soliton solution is sampled once per 20 simulation steps. The momentary Φ_ρ-ρ is obtained, and ρ_c is found by exploring the peak position of the Φ_ρ-ρ curve. The momentary energy E is given by[12]

$$E=2\pi\int_{\rho_0}^{\rho_1}\left(\frac{1}{2}\Phi_\rho^2+\frac{1}{2}\Phi_t^2+1-\cos\Phi\right)\rho\,d\rho. \tag{5}$$

At the same time, the velocity v is defined by[12]

$$v=[1-(16\pi\rho_c/E)^2]^{1/2}. \tag{6}$$

The E-ρ_c and v-ρ_c curves within a period can be obtained in this way. From Fig. 5(a) (a), one sees that the soliton energy increases approximately linearly; just after the soliton reflects at the inner boundary, the energy decreases drastically, however, its velocity decreases relatively slowly hereafter within a considerably long distance during the soliton ex-

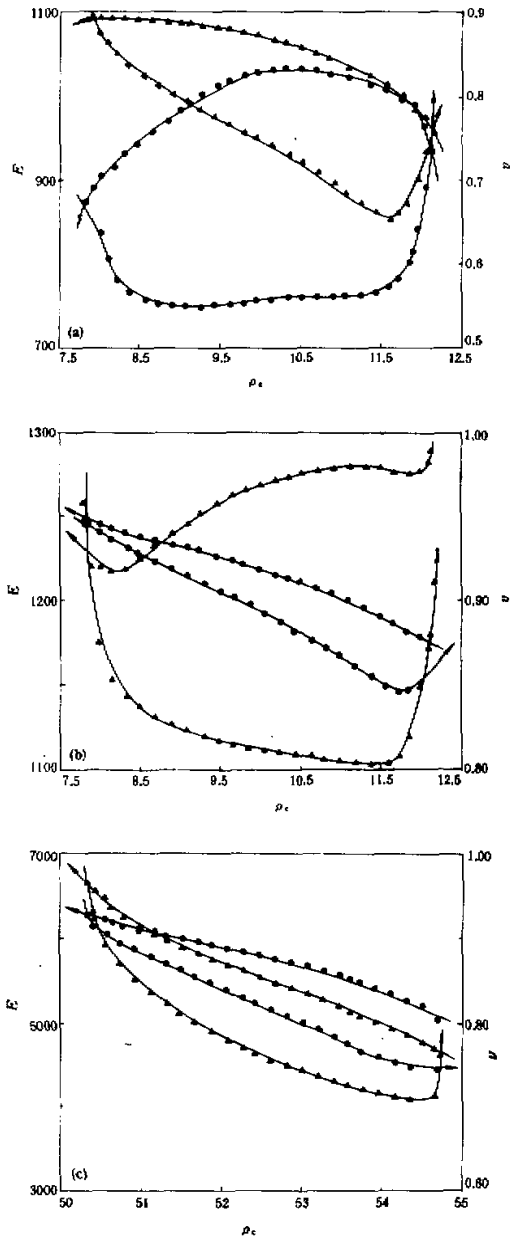

Fig. 5. Soliton center position ρ_c dependence of energy E and velocity v. (a) $\rho_0=7.5$, $\rho_1=12.5$, $\alpha=0.01$ and $F=0.068$; (b) $\rho_0=7.5$, $\rho_1=12.5$, $\alpha=0.05$ and $F=0.1600$; (c) $\rho_0=50$, $\rho_1=55$, $\alpha=0.03$ and $F=0.1600$. Triangles: E-ρ_c curve; dots: v-ρ_c curve.

panding process. E does not increase until the soliton reaches the vicinity of the outer boundary. After a reflection at the outer boundary, the soliton repeats its shrinking process. The velocity decreases during the expanding process, and increases again after the soliton collision at the outer boundary where the soliton regains much energy from the driving current. The arrows in the figure denotes the moment of reflection, and the beginning of soliton collision occurs at a distance $\Delta\rho=1$ from the outer boundary, therefore, the particle model of soliton is invalid in this situation.

However, for junctions of smaller inner radius, e. g., $\rho_0=5$ and $\rho_1=10$, the suppression effect of the dissipative term $\alpha\Phi_t$ on $1/\rho$ term is weaker. The soliton is essentially distorted, and thus a 1-ZFS that corresponds to single soliton oscillation is not likely to appear, and this has been addressed in Ref. [9].

For larger α, e.g., $\alpha=0.05$, the $1/\rho$ term and the $\alpha\Phi_t$ term compete with each other, and the latter would dominate. As long as the dissipated energy could be balanced by the energy input from the driving current, a soliton state would be stable, as shown in Fig. 3(b).

From Fig. 5 (b) one can see that the behaviour of the soliton is, in a sense, particle-like. We have chosen the same ρ_0 and ρ_1 as those in Fig. 5(a) for comparison. From Figs. 5(a) and 5(b), one can see that the variation of E and v is faster for $\alpha=0.05$ than for $\alpha=0.01$, and the collision at the outer boundary for $\alpha=0.05$ occurs at a distance $\Delta\rho=0.8$ from the outer boundary, in other words, the soliton behaves more like a particle.

For a further compariosn, we obtain in the same manner mentioned above the E-ρ_c curve and v-ρ_c curve for an annular junction with $\rho_0=50$, $\rho_1=55$, $\alpha=0.03$ and $I'=0.1600$, as shown in Fig. 5(c). The energy E and velocity v vary moderately compared with the two cases above, and the particle-like behaviour of the soliton is clear. And this is because the effect of the $1/\rho$ term is minor.

In conclusion, we find that the $1/\rho$ term and the dissipative term $\alpha\Phi_t$ in the modified SGE compete with each other for a soliton oscillation. The $1/\rho$ term dominates when the dissipation and the size of the junction is very small, e.g., $\rho_0=5$, $\rho_1=10$ and $\alpha=0.01$ (or $\alpha=0.02$), and no stable soliton oscillation exists. On the other hand, the dissipation dominates when α is relatively large and the size is small, e. g., $\rho_0=5$, $\rho_1=10$ and $0.03\leqslant\alpha\leqslant0.06$, or when α is relatively small and the size is large (for information in this respect, see Refs. [9－11]), soliton oscillation is possible if the driving current provides enough energy to compensate the dissipated energy. Therefore, the soliton behaviour depends on the inner radius in CSAJJ. As a matter of fact, for given dissipation and annular width $\rho_1-\rho_0$, there is a lower limit of inner radii for junctions to support soliton oscillation. In other words, size effect exists in this case. In addition, the lower limit of ρ_0 strongly depends on dissipation. Finally, the validity of particle model of soliton is examined, it again depends on the sizes and the dissipation of annular junctions.

ACKNOWLEDGEMENT

We are in debt to Dr. Wang Qiang-hua for his translation of the paper from its original Chinese version and some helpful suggestion he has made on the discussion in the paper.

REFERENCES

[1] A. Baron and G. Pagerno, Physics and Applications of Josephson Effect (Wiely, New York, 1982).
[2] S. N. Erne and R. D. Parmentier, *J. Appl. Phys.*, **51**(1980), 5025; D. Duchalm *et al.*, *Phys. Rev. Lett.*, **46**(1981), 1299.
[3] P. S. Lomdahl *et al.*, *Phys. Rev.*, **25B**(1982), 5737.
[4] M. P. Soerensen *et al.*, *Appl. Phys. Lett.*, **42**(1983), 793; J. J. Chang *et al.*, *Phys. Rev.*, **31B**(1985), 1658.
[5] H. G. Meyer *et al.*, *J. Appl. Phys.*, **65**(1989), 4338; S. Pagano *et al.*, *IEEE Trans. Magn.*, **25**(1989), 1080.
[6] Y. S. Kirchar and B. A. Malomed, *Rev. Mod. Phys.*, **61**(1989), 763.
[7] P. L. Christiansen *et al.*, *Appl. Phys. Lett.*, **39**(1981), 170.
[8] E. M. Maslov, *Physica*, **15D**(1985), 433; *Phys. Lett.*, **131A**(1988), 364.
[9] Xu Kun-ming, Shen Ya-fei and Yao Xi-xian, *J. Low Temp. Phys.*, **11**(1989), 187 (in Chinese); *Acta Physica Sinica*, **38**(1989), 939 (in Chinese).
[10] Xu Kun-ming, Lu Dao-fang and Yao Xi-xian, *Acta Physica Sinica*, **41**(1992), 97 (in Chinese); *J. Low temp. Phys.* **14**(1992), 293 (in Chinese).
[11] Wang Wei, A. L. Thomson and Yao Xi-xian, *Phys. Rev.*, **43B**(1991), 2756.
[12] Wang Qiang-hua, Wang Wei and Yao Xi-xian, *Acta Physica Sinica*, **40**(1991), 1999 (in Chinese); *Acta Physica Sinica*, **41**(1992), 113 (in Chinese).
[13] M. S. Dueshery *et al.*, *Phys. Rev.*, **43B**(1991), 5143.
[14] E. M. Maslov, *Teor. Mat. Fiz.*, **42**(1980), 362; (*Theor. Math. Phys.*, **42**(1980), 237).